

# RSC Advances



This is an *Accepted Manuscript*, which has been through the Royal Society of Chemistry peer review process and has been accepted for publication.

*Accepted Manuscripts* are published online shortly after acceptance, before technical editing, formatting and proof reading. Using this free service, authors can make their results available to the community, in citable form, before we publish the edited article. This *Accepted Manuscript* will be replaced by the edited, formatted and paginated article as soon as this is available.

You can find more information about *Accepted Manuscripts* in the [Information for Authors](#).

Please note that technical editing may introduce minor changes to the text and/or graphics, which may alter content. The journal's standard [Terms & Conditions](#) and the [Ethical guidelines](#) still apply. In no event shall the Royal Society of Chemistry be held responsible for any errors or omissions in this *Accepted Manuscript* or any consequences arising from the use of any information it contains.

# Synthesis, Photophysics, Ion Detection and DFT Investigation of Novel Cyano-substituted Red-light Chromophores with Triphenylamine Donor†

Na Sun, Peng Zhang\*, Yanling Hou

## Abstract

A series of novel triphenylamine-based red-light chromophores with multiple electron-withdrawing cyano substituents were synthesized by Knoevenagel condensation reaction and characterized in detail. Compounds **3-5** showed bright green-yellow emission in dichloromethane solution and red-light emission in solid state, respectively. The interesting solvatochromic behavior in different polar solvents was observed, varying from the positive solvatochromism for compound **3** to negative solvatochromism for compound **5**. In addition, the notable optical response of metal ions in DMF solution for the cyano-substituted chromophores was investigated. Especially, with the addition of  $\text{Hg}^{2+}$  ion, the blue shift in the absorption spectra and the decrease in the emission spectra suggested that the new metal complexes possibly formed between the cyano substituents and metal ions or metal ion-induced optical quenching happened. Density functional theory calculations were used to further understand the effect of the cyano substituents on the photoelectron properties of the donor-acceptor molecules.

---

\* School of Chemistry and Chemical Engineer, Southwest University, Chongqing 400715, PR China.

E-mail: ybzhang@swu.edu.cn

† Supporting Information Available: Electrochemical parameter, The thermal properties, solid morphology, photophysical properties, and metal ion detection of the compounds were available free of charge via the Internet

## Introduction

Since PPV-based light-emitting diode (LED) was reported in 1990 by Burroughes and Friend, PPV derivatives, containing polymer molecules and their oligo(phenylene vinylene), have attracted considerable attention due to their potential extensive applications, such as organic light-emitting devices<sup>1-3</sup>, solar photovoltaics<sup>4,5</sup>, field-effect transistors and biochemical sensors<sup>6,7</sup>, and so on. In the past decades, the remarkable progress in the design and development of organic photoelectron materials was made by regulating the  $\pi$ -conjugated systems or the side-chain substituents on molecular backbone<sup>8-11</sup>.

Recently, triphenylamine (TPA) has widely been introduced in the design and preparation of organic photoelectron materials due to its strong electron-donating characteristic and the modifiable molecular structure. Therefore, the organic compounds with donor- $\pi$  conjugated bridge-acceptor (D- $\pi$ -A) structure has attracted considerable interests for their broad absorption from the intramolecular charge transfer (ICT) in visible region and their lower LUMO levels<sup>12-15</sup>. For example, two starshaped D- $\pi$ -A molecules with TPA as donor, dicyanovinyl as acceptor, and 4,4'-dihexyl-2,2'-bithiophene or 4,4'-dihexyl-2,2'-bithiophene vinylene as  $\pi$ -bridge reported by J Zhang et al<sup>16</sup> possessed a broad absorption from 296 to 585 nm and lower LUMO level of -3.42 eV. In addition, optical properties of the molecules with electron accepting and donating units could be easily tuned via controlling the extent of intramolecular charge transfer (ICT). Thus, introducing stronger electron-withdrawing groups was preferable to induce efficient ICT. Cyano group as the well-known strong electron acceptor has been widely used for red-light chromophores<sup>17</sup>, which could promote the efficient ICT and enhance the exciton dipole in the excited state<sup>18-20</sup>. In particular, introducing multi-cyano groups into a conjugated system resulted in stronger electron-accepting effect<sup>21-23</sup>. So far, the TPA-based compounds with D- $\pi$ -A structure and multi-cyano groups as the electron acceptor have been reported. For example, the new TPA-based compounds with tetracyanoethylene groups reported by Mircea Grigoras showed the board absorption

over the solar spectrum<sup>24</sup>, which were the desirable candidates for bulk-heterojunction and dye-sensitized solar cells. Yang Yang et al reported the multi-branched TPA derivatives with dicyanovinyl as electron acceptor, presenting the outstanding solvatochromic behaviors<sup>25</sup>. Besides, the optical probe of the TPA-based chromophores was recently reported as due to the coordination of metal ions by cyano groups<sup>26</sup>. Consequently, the introduction of cyano substituents on the TPA-based derivatives could finely tune the electron energy levels.

In this report, the synthesis, photophysical performances and electron structures of novel D- $\pi$ -A molecules with TPA as donor, cyano groups as acceptor, and the ethynylbenzene units as the  $\pi$ -conjugated linkage were investigated systematically. Cyano substituents on the conjugated system could facilitate tuning the optical properties. These compounds do show red-emitting in solid as expected, and possess broad visible absorption band. Furthermore, theoretical calculation was performed to further understand the effect of the cyano substituents on the TPA-based molecules on the optical properties.

## Experimental section

### Materials

Triphenylamine (TPA), Potassium tert-butoxide (t-BuOK), N-bromosuccinimide (NBS), CuCN, Malononitrile, metal salts ( $\text{Hg}(\text{CH}_3\text{COO})_2$ ,  $\text{SnCl}_2 \cdot 2\text{H}_2\text{O}$ , and so on) are commercial products from Aldrich and were directly used without further purification. Solvents such as triethylamine, dimethylformamide (DMF), phosphorus oxychloride ( $\text{POCl}_3$ ) and tetrahydrofuran (THF) were purchased from commercial sources. Compound 1,4-dibromo-2,5-bis(diphenylaminophenyl) benzene (**1**) was synthesized according to the literature reported<sup>27</sup>.

### General characterization

$^1\text{H}$  and  $^{13}\text{C}$  NMR spectra were recorded with a Bruker Avance III 600 MHz spectrometer. ESI-TOF MS data were performed on a Bruker esquire 2000 mass system. The infrared (IR) spectra were measured on a Shimadzu FTIR-8400 spectrometer with KBr pellets. X-ray diffraction (XRD) was carried out on an XD-3

powder diffractometer (Purkinje General Instrument Co., Beijing, China). Scanning electron microscope (SEM) images were observed by an S4800 (Hitachi, Japan) at 20kV. The thermal behaviors of these compounds were performed with a TA SDTQ600 thermal gravimetric analyzer (TGA, USA) and differential scanning calorimetry (DSC, Model 200F3-Maia, Germany) under a dry nitrogen gas flow at a heating rate of 10 °C/min. Ultraviolet-visible absorption (UV-vis) and emission spectra in solution, thin film and powder were performed on a UV-2550 spectrometer (Shimadzu, Japan) and F-7000 fluorescence spectrometer (Hitachi, Japan). The fluorescence quantum yield of these compounds in different polar solvents at room temperature was recorded using FL-TCSPC time resolved fluorescence spectrometer (HoribaJobin Yvon Inc, France). The luminescence decay lifetimes were recorded using fluorescence lifetime spectrometer (FL-TCSPC Horiba, Jobin Yvon Inc, France). Cyclic voltammetry was recorded on a CHI-660D electrochemical workstation (Chenghua Co., China) with platinum wire as counter electrode, Pt as working electrode and saturated calomel electrode as reference electrode, respectively. Theoretical calculation was performed with time dependent density functional theory (TD-DFT, B3LYP/6-31G (d)) on Gaussian 09 quantum chemical program package.

#### **Synthesis of triphenylamine-malononitrile derivatives 2-5**

**4,4((((1E,1'E)-2,5-dibromo-1,4-phenylene)bis(ethene-2,1-diyl)bis(4,1-phenylene))-bis(phenylazanediy))dibenzaldehyde (compound 2):** POCl<sub>3</sub> (2.4mL, 25.75 mmol) was dropwise added at 0°C to 1,4-dibromo-2,5-bis(diphenylamino-phenyl)benzene (1.6 g, 2.06 mmol) in dry DMF solution, and the mixture was heated and kept at 90°C for 12 h. Then POCl<sub>3</sub> (1.2 mL, 12.88 mmol) was added again and reacted for 12 h. After the reaction, the mixture was cooled to room temperature, poured into ice water, and neutralized with aqueous 2M NaOH solution in turn. And then the solvent was removed under a reduced pressure. The residue was washed with distilled water and separated by column chromatography (silica gel, petroleum ether/EtOAc, 6:1, v/v). Finally, the product was obtained as yellow powder (1.43 g, 83% yield). <sup>1</sup>H NMR (600 MHz, CDCl<sub>3</sub>) : δ (ppm) : 9.84 (s, 2H), 7.87(s, 2H), 7.72 (d, J = 6.0Hz, 4H), 7.52(d, J =8.4Hz, 4H), 7.38-7.35 (m, 4H), 7.33 (d, J = 16.2Hz, 2 H), 7.2-7.19(m, 6H),

7.17 (d, J=9Hz, 4H), 7.10 (d, J=6Hz, 4H), 7.05 (d, J=16.2Hz, 2H). ESI-TOF MS: Calcd for C<sub>48</sub>H<sub>34</sub>Br<sub>2</sub>N<sub>2</sub>O<sub>2</sub> 828.1; found: 828.5.

**2,5-bis(4-((4-formylphenyl)(phenyl)amino)styryl)terephthalonitrile(compound 3):**

The mixture of compound **2** (0.5 g, 0.6 mmol), and CuCN (0.14 g, 1.5 mmol) were dissolved in 50 mL DMF under nitrogen atmosphere and stirred at 155 °C for 48 h. The reaction mixture was cooled to room temperature (RT), poured into water, filtered, washed with ammonia (15%) and water in turn. And then, the residue was purified with column chromatography (silica gel, petroleum ether/EtOAc, 6:1, v/v). Finally, the compound **3** was obtained as yellow powder (0.32 g, 73% yield). <sup>1</sup>H NMR (600 MHz, CDCl<sub>3</sub>) : δ (ppm) : 9.88 (s, 2H), 8.05(s, 2H), 7.77 (d, J = 8.4Hz, 4H), 7.57(d, J = 9Hz, 4H), 7.42-7.39 (m, 4H), 7.32 (d, J = 6Hz, 4 H), 7.22 ( d, J=6Hz, 2H), 7.21-7.2(m, 8H), 7.15 (d, J=8.4Hz, 4H). <sup>13</sup>C NMR (150 MHz, CDCl<sub>3</sub>) δ 190.4, 152.7, 147.5, 145.9, 138.9, 134.2, 131.5, 131.3, 130.2, 130.0, 129.7, 128.7, 126.6, 125.6, 125.2, 121.1, 120.9, 116.6, 114.9. ESI-TOF MS: Calcd for C<sub>50</sub>H<sub>34</sub>N<sub>4</sub>O<sub>2</sub> 722.2; found: 722.7. FT-IR(KBr)v,cm<sup>-1</sup>: 3032(=C-H), 2221(-C≡N), 1686(C=O), 1585, 1581(C=C), 1285(C-N), 1319, 1165(C-CN), 964, 822, 698(C-H).

**2,2'-(4,4'-(4,4'-(1E,1'E)-2,2'-(2,5-dicyano-1,4-phenylene)bis(ethene-2,1diyl)bis(4,1-phenylene))bis(phenylazanediy)bis(4,1-phenylene))bis(methan-1-yl-1-ylidene)**

**dimalononitrile(compound 4):** Compound **3** (0.32 g, 0.44 mmol) in anhydrous DCM (30 mL) was added malononitrile (0.64 g, 0.97 mmol) at RT and 5 drops of triethylamine were added. After stirred 24h at RT, the reaction mixtures were concentrated and purified with column chromatography (silica gel, petroleum ether/EtOAc, 6:1, v/v) to obtain the compound **4** as red powder (0.25 g, 69% yield).

<sup>1</sup>H NMR (600 MHz, CDCl<sub>3</sub>) : δ (ppm): 7.91 (s, 2H), 7.80(d, J = 3Hz , 4 H), 7.58(d, J = 7.2Hz, 4H)7.56(s, 2 H), 7.44-7.42 (m, 4H),7.38 (d, J = 16.2Hz, 2H), 7.24-7.21(m, 6H)7.22 (d, J = 8.4Hz, 4H), 7.06 (d, J = 9Hz, 2H), 7.04 ( d, J=9Hz, 4H). <sup>13</sup>C NMR (150 MHz, CDCl<sub>3</sub>) δ 157.8, 152.8, 146.4, 145.0, 134.1, 132.9, 130.2, 129.8, 128.8, 128.7, 128.5, 126.9, 126.5, 126.2, 126.0, 123.8, 121.8, 119.8, 119.5, 115.1, 113.8. ESI-TOF MS: Calcd for C<sub>56</sub>H<sub>34</sub>N<sub>8</sub> 818.2; found: 817.7. FT-IR(KBr)v,cm<sup>-1</sup>: 3032 (=C-H), 2218(-C≡N), 1568, 1500, 1323(C=C), 1292(C-N), 1184(=C-CN), 960, 822,

694(C-H).

**2,2'-(4,4'-(4,4'-(1E,1'E)-2,2'-(2,5-dibromo-1,4-phenylene)bis(ethene-2,1-diyl)bis(4,1-phenylene))bis(phenylazanediy)bis(4,1-phenylene))bis(methan-1-yl-1-ylidene) dimalononitrile(compound 5):** A solution of compound **2** (0.5 g, 0.6 mmol) in anhydrous DCM (30 mL) was added malononitrile (0.87 g, 1.32 mmol) at RT to which was added 8 drop triethylamine. After stirred 24h at RT, the reaction mixtures were concentrated and purified with column chromatography (silica gel, petroleum ether/EtOAc, 6:1, v/v) to yield the compound **5** as red powder (0.38 g, 68% yield). <sup>1</sup>H NMR (600 MHz, CDCl<sub>3</sub>) : δ (ppm) : 7.91 (s, 2H), 7.80(d, J = 8.4Hz , 4H), 7.58(d, J = 6.6Hz , 4H)7.57(s, 2H), 7.44-7.42 (m, 4H), 7.38 (d, J = 16.2Hz, 2H), 7.24-7.21(m, 6H)7.23 (d, J = 1.2Hz, 4H), 7.06 ( d, J= 9Hz, 4H),7.05 (d, J = 6Hz, 2H). <sup>13</sup>C NMR (150 MHz, CDCl<sub>3</sub>) δ 157.8, 153.1, 145.4, 145.1, 137.4, 134.1, 133.0, 131.2, 130.4, 130.1, 128.4, 126.8, 126.4, 126.3, 126.0, 123.4, 123.1, 119.3, 115.0, 113.9. ESI-TOF MS: Calcd for C<sub>54</sub>H<sub>34</sub>Br<sub>2</sub>N<sub>6</sub> 922.1; found: 921.6. FT-IR(KBr)v,cm-1: 3032(=C-H), 2218(-C≡N), 1566, 1497, 1323(C=C), 1296(C-N), 1184(=C-CN), 1053, 814, 694(C-H).

## Results and discussion

### Thermal Properties and Morphology

In order to evaluate the thermal properties of the compounds **3-5**, their thermo-gravimetric analysis (TGA) and differential scanning calorimetry (DSC) were carried out under a nitrogen atmosphere and the corresponding data were summarized in Table 1. As shown in Fig.S1, TGA results exhibited that the degradation temperatures (Td) of the compounds **3-5** were 350°C, 390°C and 390°C (5% weight loss), respectively, the higher degradation temperatures of compounds **4** and **5** were attributed to multi-cyano end substitutes which resulted in the strong intramolecular interaction. It demonstrated that thermal stability of the compounds was regulated by the amount and position of the cyano substituents. In addition, DSC (Fig.S2) analysis indicated that the compounds only showed a relative weak endothermic step-transition in the scanning region, which could be attributed to the glass phase transition. The

glass transition temperature of the compounds **3-5** was 111°C, 116°C and 108°C, respectively. From the above data it was obvious that the cyano-substituted compounds provided with a certain amorphous characteristic.

In order to further evaluate the morphologic nature of the compounds in solid state, the morphologic investigations have been performed using the powder X-ray diffraction analysis (XRD). As shown in Fig.S3, a series of sharp peaks for compound **3** were observed owing to the restriction in molecular ordered aggregation and crystallinity by terminal aldehyde groups<sup>28</sup>. Meanwhile, compound **4** showed a sharper peak, which demonstrated that end multi-cyano substituted molecules showed the crystallization tendency in solid state. However, compound **5** displayed a series of more intensive peaks, comparing to those of the first two compounds, demonstrating the difference in the crystal phase or intermolecular interaction in the solid state. Furthermore, The XRD profile of compound **4** showed one strong peak ( $d=1.022$  nm) in the small-angle region except for several weak peaks in the wide-angle region (Fig.S3). Compound **3** exhibited the similar XRD profiles, which were consisted of one strong peak ( $d=0.883$  nm) in the small-angle region and a series of relative strong peaks in the wide-angle region, indicating the similar packing mode of compound **4**. In contrast, the XRD profile of compound **5** exhibited a series of relatively strong peaks in the small- and wide-angle region, which one strongest peak in the small-angle region ( $d=1.061$  nm) and wide-angle region ( $d=0.408$  nm), respectively.

### Photophysical Properties

The UV-vis absorption and photoluminescence spectra of compounds **3-5** in dichloromethane solution were displayed in Fig.1 and the corresponding photophysical data were summarized in Table 1. All novel synthesized chromophores, containing two electron-donating TPA terminals and bis(styryl)benzene backbone, presented two distinct absorption bands around 260 nm and 470 nm. The absorption around 260 nm was attributed to a  $\pi-\pi^*$  or  $n-\pi^*$  transition on the TPA donor, while the absorption around 470 nm was assigned to the intramolecular charge transfer (ICT) from the TPA donor to the centre bis(styryl)benzene backbone acceptor except for the contribution of cyano substituents. In addition, it should be noted that the weak

absorption at about 320 nm was observed for the compounds, probably owing to the combined effect of  $\pi-\pi^*$  transition of the molecular backbones and the electron-withdrawing cyano substituents on the TPA parts<sup>29</sup>.

In addition, the absorption spectra of the compounds showed red shift compared with that of their TPA-based analogues without cyano substituents reported in the literatures (410 nm)<sup>30</sup>. The lower energy absorption band for compound **3** was around 439 nm. Compounds **4** and **5** presented more remarkable red shift in absorption maximum than compound **3** (30nm and 24nm, respectively), probably attributing to the stronger influence of cyano substituent on terminal TPA parts in comparison with those on the center benzene ring. All of the compounds displayed relatively strong green-light emission in solution. Obvious red-shift emission of compound **4** was attributed to the combined effect of cyano substituents on different benzene rings compared with compounds **3** and **5**. In addition, compounds **4** and **5** showed lower PL quantum efficiencies, which suggested that the effect of terminal cyano substituents on TPA units maybe resulted in the more nonradiative transitions of the compounds (Table 1).

Compared with UV-vis absorption and emission spectra in solution, compounds **3-5** in thin film exhibited the larger red-shift, and broad and structureless absorption bands, demonstrating strong intermolecular  $\pi-\pi^*$  interaction or aggregation in solid state(Fig.2). Compound **3** showed bright orange fluorescence (572 nm) in thin film, while compounds **4** and **5** showed red emission at 609 and 608 nm in thin film. In addition, the red fluorescence for compounds **4** and **5** were observed at 619 and 623 nm in powder state, respectively, indicating more remarkable red-shift, which demonstrated much stronger intermolecular  $\pi-\pi^*$  interaction or aggregation in powder state than in film (Fig.S4 and Fig.S5).

Moreover, the concentration dependence of the emission of the compounds in dichloromethane solution was also investigated (Fig.3 and Fig.S6). As shown in Fig.3, the emission spectra of the compound **5** showed notably red shift except for the concentration quenching with increasing the solution concentration. It demonstrated that the intermolecular  $\pi-\pi^*$  interaction or aggregation was present in high solution

concentration.

The solvatochromism of the novel red compounds was assessed in different polar solvents. As shown in Fig.S7, the absorption maxima of these TPA derivatives showed the slightly negative solvatochromism with the increase of solvent polarities. In other words, compound **3** exhibited blue-shifted absorption with increasing the solvent polarity, shorter wavelength absorption maxima in DMF (435 nm) and longer wavelength in TOL (445 nm) (Table 2). Similarly, compounds **4** and **5** showed a red-shifted absorption maxima in non-polar TOL solvent (464 and 458 nm) and blue-shifted absorption maxima in polar DMF solvent (460 and 436 nm), respectively. The results suggested that the dipole moment of the molecules in the excited state was decreased due to the effect of electron-withdraw cyano substituents.

Furthermore, the emission solvatochromism of the compounds was examined with the increase of solvent polarity from non-polar solvent (toluene) to polar solvent (DMF) (Fig.4 and Fig.S8). Interestingly, varying from non-polar solvent to polar solvent, the emission spectra of compound **3** showed progressively red-shift (515 nm in TOL solutions and 556 nm in DMF solutions) and the emission broadening (Fig.4a), indicating that the intramolecular charge transfer (ICT) occurred in the excited state from electron donor to electron acceptor. However, compound **4** only showed weaker positive solvatochromism with the increase of solvent polarity. This suggested that the combined effect of cyano substituents on the different positions weakened ICT abilities in the excited state (Fig.4b). In contrast, compound **5** indicated obviously negative solvatochromism, blue shift of 36 nm as the solvent polarity varied from non-polar solvent to polar solvent (Fig.4c). The result implied that solvent polarity-induced distortion of molecular planarity restricted the intramolecular charge transfer transition, resulting in the blue-shift emission<sup>31</sup>.

The linear variety of Stokes shift of the compounds **3-5** to Lippert–Mataga solvent polarity parameter,  $\Delta f$ ,<sup>32</sup> was plotted in Fig.4d. Compound **3** showed an obvious increase of Stokes shift along with increase of  $\Delta f$ , suggesting that it provided with strong ICT characteristic in the excited state. For compound **4**, the fit line relationship between Stokes shift and  $\Delta f$  had a comparably gentle slope and exhibited

a slight deviation in the experimental data. This suggested that compound **4** underwent a small dipolar change in the excited process from non-polar to polar solvent. In contrast, the slope value of the line relationship for compound **5** was negative, which demonstrated that compound **5** had a negative solvatochromism. In a word, the ICT character of compounds **3-5** could be tuned by terminal cyano.

Fluorescence quantum yields ( $\Phi_F$ ) of compounds **3-5** were studied in different solvents to get a deep understanding on the solvatochromism behavior. The  $\Phi_F$  of compound **3** was observed as high as 0.765 in low polar solvent of toluene (Table 2), and gradually decreased with the increase in polarity, indicating that the strong solvent polarity could result in the increase in the nonradiative transition. However, compounds **4** and **5** exhibited the relatively higher  $\Phi_F$  in high polar solvents, while only lower  $\Phi_F$  was observed in nonpolar solvent, demonstrating that the cyano substituents on TPA units were not bad for the  $\Phi_F$ .

Luminescence decay lifetimes of compounds **3-5** were performed in dichloromethane solution (Table. 1). Compound **3** (2.68ns) exhibited the relatively higher Luminescence decay lifetime than compounds **4** and **5** (1.58ns and 1.86ns), demonstrating that introducing the cyano substituents to TPA units led to an enhanced ICT character which changes the decay of the singlet excited states. Actually, the high strength ICT led to the increase of intramolecular rotation and the distortion which increased the energy loss of the nonradiative transition, and thus the Luminescence decay lifetime was decreased.

### **Metal Ion Detection**

The cyano substituents on the compounds were able to form coordination complex with metal ions<sup>33</sup>. Therefore, in order to explore the potential application of these compounds, the effect of the addition of metal ions on the optical properties of compounds **3-5** was recorded in DMF solution (Fig.S9-S11). The results indicated that the presence of the metal ions, including  $\text{Ba}^{2+}$ ,  $\text{Co}^{2+}$ ,  $\text{Cr}^{3+}$ ,  $\text{Cu}^{2+}$ ,  $\text{Hg}^{2+}$ ,  $\text{Pb}^{2+}$ ,  $\text{Sn}^{2+}$  and  $\text{Zn}^{2+}$ , could cause the change in the absorption and emission spectra, deviating from the initial positions. The compounds **4** and **5** showed hypsochromic shift in the absorption spectra to a certain extent and an increase or a decrease in the emission

spectra with the addition of metal ions.

The metal ion  $\text{Hg}^{2+}$  was chosen as an example to further assess the influence of metal ion on the absorption and emission spectra of compounds **3-5**. The concentration of compounds **3-5** was fixed at  $1 \times 10^{-5}$  M/L and the metal ion concentration varied from  $1 \times 10^{-4}$  to  $9 \times 10^{-4}$  M/L. The UV-vis absorption and PL spectra were recorded immediately after the addition of metal ions (Fig.5 and Fig.S12). The absorption and emission maximum of compound **3** in DMF solution only displayed a gradual decrease without notable red shift, with the addition of  $\text{Hg}^{2+}$  up to the concentration of  $9 \times 10^{-4}$  mol/L, which may be attributed to the  $\text{Hg}^{2+}$  ion-induced decrease in the ICT band.

In case of cyano-substituted TPA derivatives, the absorption spectra of compounds **4** and **5** showed the remarkable hypsochromic shift and a new peak appeared at around 330 nm after  $\text{Hg}^{2+}$  ions were added. Simultaneously, with increasing  $\text{Hg}^{2+}$  ions, the peak intensity of the absorption spectra decreased. The results may be attributed to a result of ICT between the electron-withdrawn cyano and electron-donor TPA units by  $\text{Hg}^{2+}$  ions inducing, or the new coordinative complex possibly formed between cyano groups and  $\text{Hg}^{2+}$  ions. In addition, the presence of  $\text{Hg}^{2+}$  ions had a certain influence on the emission intensity, which presented firstly an increase, and then a decrease as the  $\text{Hg}^{2+}$  ions increased.

### Electrochemical properties

The electrochemical behaviors of the compounds **3-5** were studied using cyclic voltammetry (CV) in dimethylformamide (DMF) in the presence of tetrabutylammonium perchlorate (TBAP) as a supporting electrolyte (Fig.6, Table 3 and Table S1 in Supporting Information). The CV curves of the compounds exhibited an irreversible oxidation process in the positive scanning region and several successive irreversible reduction processes in the negative scanning region, which were assigned to the oxidation of TPA units and the reduction of the combination of the conjugated distyrylbenzene core and cyano substituents, respectively. The anodic scanning showed an onset oxidation potential of 0.97 V for compounds **3**, 0.99 V for compound **4** and 0.96 V for compound **5**, respectively. In contrast, compounds **3-5**

provided with an onset reduction potential of -1.38, -1.30 and -1.36 V, respectively. According to equations reported in the literature<sup>34</sup>, The energy levels of the highest occupied molecular orbital (HOMO) and lowest unoccupied molecular orbital (LUMO) and the electrochemical band gap (Eg) of compound **3** were estimated to be -5.67, -3.32 and 2.35 eV, respectively. Similarly, for compound **5**, the HOMOs, the deeper LUMOs and the corresponding Eg were obtained at -5.66 eV, 3.34 eV and 2.32 eV, respectively. While compound **4** possessed the deeper HOMOs (-5.69 eV) and LUMOs levels (-3.40 eV), resulting in the narrower band gap (2.29 eV), due to the presence of the more electron-withdrawing cyano substituents on TPA parts. The electrochemical band gaps of compound **3-5** were in agreement with the optical measurements. Consequently, the electron structures of the synthesized compounds succeeded in being fine-tuned by the cyano substituent on the TPA-based derivatives.

#### DFT Investigation

In order to further clarify the experimental results, the space geometries of compounds **3-5** were optimized as shown in Table 4, and the corresponding parameters were summarized in Table 5. Compounds **3-5** showed a slight twist along the conjugated distyrylbenzene skeleton, respectively (Table 5). The small twist dihedral angles along C<sub>5</sub>-C<sub>6</sub>-C<sub>9</sub>-C<sub>10</sub> and C<sub>9</sub>-C<sub>10</sub>-C<sub>19</sub>-C<sub>20</sub> for compound **3** were 2.20° and 2.67°, respectively. While compound **4** presented the smaller twist dihedral angles (1.10° and 2.01°) along C<sub>5</sub>-C<sub>6</sub>-C<sub>9</sub>-C<sub>10</sub> and C<sub>9</sub>-C<sub>10</sub>-C<sub>19</sub>-C<sub>20</sub> due to the combined influences of cyano substituents in the middle and terminal region. Interestingly, larger twist dihedral angles along C<sub>5</sub>-C<sub>6</sub>-C<sub>7</sub>-C<sub>8</sub> and C<sub>16</sub>-C<sub>15</sub>-C<sub>8</sub>-C<sub>7</sub> for terminal cyano-substituted compound **5** were 13.93° and 5.57°, in agreement with the optical characteristics. Moreover, the three phenyl rings on TPA group displayed different twist dihedral angles each other. The twist dihedral angles among three rings on TPA decreased from -73.80° to -79.64° along C<sub>23</sub>-C<sub>24</sub>-C<sub>26</sub>-C<sub>28</sub> (for compounds **3** and **4**) or C<sub>19</sub>-C<sub>20</sub>-C<sub>22</sub>-C<sub>24</sub> (for compound **5**). While twist dihedral angles increased from -63.10° to -61.26° along C<sub>21</sub>-C<sub>24</sub>-C<sub>32</sub>-C<sub>35</sub> (for compounds **3** and **4**) or C<sub>17</sub>-C<sub>20</sub>-C<sub>28</sub>-C<sub>31</sub> (for compound **5**) and -71.24° to -67.80° along C<sub>27</sub>-C<sub>26</sub>-C<sub>32</sub>-C<sub>33</sub> (for compounds **3** and **4**) or C<sub>23</sub>-C<sub>22</sub>-C<sub>28</sub>-C<sub>29</sub> (for compound **5**), respectively. Similar alteration in plane angle for

compounds **3-5** has been given in Table 5. Thus, such varieties further confirmed the effect of electron-withdrawn cyano substituents on molecular space geometries.

The HOMO and LUMO for compounds **3-5** were plotted in Table 4. The HOMO was delocalized over the entire molecule, while the LUMO was mainly localized on the center conjugated moieties through the  $\pi$ -bridge. In addition, the LUMO for compounds **4** and **5** extended the terminal-substituted cyano branches on the TPA moieties. Especially, for compound **5**, the terminal-substituted cyano presented the stronger influence on the LUMO, which further verified that the charge distribution on such molecules was extremely influenced by terminal cyano. The results would lead to the difference in the photophysical properties among compounds **3-5** when the intramolecular charge transfer happened during an excited process.

The HOMO energy levels ( $E_{\text{HOMO}}$ ), LUMO energy levels ( $E_{\text{LUMO}}$ ) had been estimated in Table 4. The  $E_{\text{HOMO}}$  and  $E_{\text{LUMO}}$  for the compound **3** were -5.28 and -3.01eV, respectively. Introducing the electron-withdrawing cyano on the benzene ring resulted in a remarkably low  $E_{\text{LUMO}}$  as increasing number of cyano group. Compared with compound **3**, introducing dicyanovinyl arms on TPA parts for compound **4** resulted in lower  $E_{\text{HOMO}}$  and  $E_{\text{LUMO}}$  energies. However, in comparison with compound **4**, compound **5** exhibited a slight increase in  $E_{\text{HOMO}}$  and  $E_{\text{LUMO}}$  due to the absence of cyano substituents on the phenyl core, which was in agreement with those from electrochemical experiment. In a word, the cyano substituents on TPA-based derivatives could finely regulate the electron structures, resulting in the red-light properties.

## Conclusion

In this work, three new TPA-based chromophores with electron-drawing cyano substituents were synthesized. Their relevant characterizations were performed by TGA, DSC, UV-vis, PL spectroscopy and cyclic voltammetry. Compounds **3-5** showed bright green-yellow emission in dichloromethane solution and red-light emission in solid state, respectively. Interestingly, compounds **3** and **4** showed the significant positive solvatochromism and the weaker positive solvatochromism with

increasing the polarity of solvent, respectively, while the negative solvatochromism for compound **5** was observed, owing to the effect of terminal cyano substituents. Furthermore, the compounds showed the optical response to metal ions. Especially, by the change of  $\text{Hg}^{2+}$  concentration, the blue shift in the absorption spectra and the decrease in the emission intensity demonstrated that the compounds were the potential materials as highly selective and sensitive optical sensors. The electrochemical characterization and DFT calculation validated the fine regulation in the HOMO and LUMO from the variety of cyano substituents. In addition, DFT calculation revealed the essence that the cyano substituents regulated the photophysical properties, electrochemical characteristics and electron structures of the donor-acceptor molecules.

### Acknowledgement

We gratefully acknowledged the Fundamental Research Funds for the Central Universities (XDJK2015C020) for the financial support.

### Notes and references

- 1 X. Zhang, B. Chen, X. Lin, O. Wong, C. Lee, H. Kwong, S. Lee and S. Wu, *Chem. Mater.*, 2001, **13**, 1565-1569.
- 2 C. Y. B. Ng, K. H. Yeoh, T. J. Whitcher, N. A. Talik, K. L. Woon, T. Saisopa, H. Nakajima, R. Supruangnet, P. Songsiriritthigul, *J. Phys. D Appl. Phys.*, 2014, **47**, 015106.
- 3 M. Belhaj, C. Dridi, H. Elhouichet, *J. Lumin.*, 2015, **157**, 53-57.
- 4 J. Huang, C. Li, Y. J. Xia, X. H. Zhu, J. Peng, Y. Cao, *J. Org. Chem.*, 2007, **72**, 8580-8583.
- 5 N. Tamoto, C. Adachi, K. Nagai, *Chem. Mater.*, 1997, **9**, 1077-1085.
- 6 T. Lei, X. Xia, J. Y. Wang, C. J. Liu, J. Pei, *J. Am. Chem. Soc.*, 2014, **136**, 2135-2141.
- 7 D. Zhao, J. Du, Y. Chen, X. Ji, Z. He and W. Chan, *Macromolecules*, 2008, **41**, 5373-5378.
- 8 E. Cevik, D. İlicalı, D. A. M. Egbe, S. Günes, *Sol .Energ.Mat.Sol .C*, 2012, **98**, 94-102.

- 9 B. Stender, S. F. Völker, C. Lambert, J. Pflaum, *Adv. Mater.*, 2013, **25**, 2943-2947.
- 10 A. G. Del Mauro, M. GraziaáMaglione, *J. Mater. Chem. C*, 2015, **3**, 147-152.
- 11 S. T. Iacono, S. M. Budy, J. D. Moody, R. C. Smith, D. W. Smith Jr, *Macromolecules*, 2008, **41**, 7490-7496.
- 12 X. Mei, G. Wen, J. Wang, H. Yao, Y Zhao, Z. Lin, Q. Ling, *J. Mater. Chem. C*, 2015, **3**, 7267--7271
- 13 M. Aydemir, G. Haykır, F. Tu`rksoy, S. Gu`mu`s, F. B. Diasa, A. P. Monkman, *Phys. Chem. Chem. Phys.*, 2015, 17, 25572-25582.
- 14 S. H. Kim, J. Choi, C. Sakong, J. W. Namgoong, W. Lee, D. H. Kim, B. Kim, M. J. Ko, J. P. Kim, *Dyes and Pigments*, 2015, **113**, 390-401.
- 15 F. Wu, S. Zhao, L. T. L. Lee, M. Wang, T. Chen, L. Zhu, *Tetrahedron Lett.*, 2015, **56**, 1233-1238.
- 16 J. Zhang, D. Deng, C. He, Y. He, M. J. Zhang Z. G. Zhang, Z. J. Zhang, Y. F. Li, *Chem. Mater.*, 2011, **23**, 817-822.
- 17 X. Liu, Z. Cao, H. Huang, X. Liu, Y. Tan, H. Chen, Y. Pei, S. Tan, *J. Powder Sources*, 2014, **248**, 400-406.
- 18 Z. M. Ju, H. L. Jia, X. H. Ju, X. F. Zhou, Z. Q. Shi, H. G. Zheng, M. D. Zhang, *RSC Adv.*, 2015, **5**, 3720-3727.
- 19 Z. G. Zhang, Y. Yang, S. Zhang, J. Min, J. Zhang, M. Zhang, X. Guo, Y. Li, *Synth. Met.*, 2011, **161**, 1383-1389.
- 20 X. Tang, W. Liu, J. Wu, C. S. Lee, J. You, P. Wang, *J. Org. Chem.*, 2010, **75**, 7273-7278.
- 21 V. Jeux, O. Segut, D. Demeter, O. Alévêque, P. Leriche, J. Roncali, *Chem Plus Chem.*, 2015, **80**, 697-703.
- 22 F. Tancini, Y. L. Wu, W. B. Schweizer, J. P. Gisselbrecht, C. Boudon, P. D. Jarowski, M. T. Beels, I. Biaggio and F. Diederich, *Eur. J. Org. Chem.*, 2012, **14**, 2756-2765.
- 23 W. Huang, F. Tang, B. Li, J. Sua, H. Tian, *J. Mater. Chem. C*, 2014, **2**, 1141-1148.
- 24 M. Grigoras, T. Ivan, L. Vacareanu, A. M. Catargiu and R. Tigoianu, *J. Lumin.*, 2014, **153**, 5-11.
- 25 Y. Yang, B. Li, L. Zhang, *Sensor Actuat B Chem.*, 2013, **183**, 46-51.

- 26 W. Shi, F. Ma, Y. Hui, H. Mi, Y. Tian, Y. Lei, Z. Xie, *Dyes and Pigments*, 2014, **104**, 1-7.
- 27 P. Liu, P. Zhang, D. Cao, L. Gan and Y. Li, *J.Mol.Struct.*, 2013, **1050**, 151-158.
- 28 Q. Fang, T. Yamamoto, *Macromolecules*, 2004, **37**,5894-5899.
- 29 D.S. Leem, K.H. Lee, K.B. Park, S.J. Lim, K.S. Kim, Y. Wan Jin and S. Lee, *Appl.Phys.Lett.*, 2013, **103**, 043305.
- 30 L. Dong, G. Li, A. D. Yu, Z. Bo, C. L. Liu and W. C. Chen, *Chem Asian.J.*, 2014, **9**, 3403-3407.
- 31 E. C. H. Kwok, D. P. K. Tsang, M. Y. Chan, V. W. W. Yam, *Chem. Eur. J.*, 2013, **19**, 2757-2767.
- 32 S. Y. Kim, Y. J. Cho, G. F. Jin, W. S. Han, H. J. Son, D. W. Cho, S. O. Kang, *Phys. Chem. Chem. Phys.*, 2015, **17**, 15679-15682.
- 33 L. Vacareanu, I. Teofilia, M. Grigoras, *Macromol. Res.*, 2013, **21**, 1059-1068.
- 34 L. Liu, H. Li, J. Bian, J. Qian, Y. Wei, J. Li and W. Tian, W., *New. J. Chem .*, 2014, **38**, 5009-5017.

## Table and Figure Captions

**Table.1** The data of photophysical and thermal properties of compounds **3-5**

**Table.2** Data of optical properties of compounds **3-5** in different polar solvent

**Table.3** The electrochemical data and energy levels of the compounds **3-5**

**Table.4** The electronic structure data by the theoretic calculation of compounds **3-5**

**Table.5** Optimized geometry parameters of bond lengths, bond angles and dihedral angles for compounds **3-5**(bond lengths are in Å, bond angles and dihedral angles)

**Scheme 1.** Synthetic routes for compounds **3-5**

**Fig.1** Normalized UV-vis absorption and emission spectra of compounds **3-5** in dichloromethane solution ( $1 \times 10^{-5} \text{M}$ )

**Fig.2** UV-vis absorption and PL emission spectra of compounds **3-5** in thin film

**Fig.3** The concentration dependence of the emission spectra of compound **5** in dichloromethane solution (mol/L)

**Fig.4** Normalized emission spectra of compounds **3-5** in different polar solvents and solvatochromatic shift

**Fig.5** Absorption spectra of the compounds **3-5** in DMF ( $1 \times 10^{-5} \text{M/L}$ ) with the addition of  $\text{Hg}^{2+}$  in DMF solution ( $1 \times 10^{-4} \text{M/L}$ )

**Fig.6** Cyclic voltammetry of compounds **3-5** in DMF solution at the scanning rate of 100 mV/s

**Table. 1**

Compds	$\lambda_{\text{abs}}/\text{nm}$ (Sol)	$\lambda_{\text{em}}/\text{nm}$ (Sol)	$\lambda_{\text{abs}}/\text{nm}$ (Film)	$\lambda_{\text{em}}/\text{nm}$ (Film)	$\lambda_{\text{em}}/\text{nm}$ (solid)	$T_g$ (°C)	$T_d$ (°C)	<sup>a</sup> $\tau$ (ns)
<b>3</b>	439	542	458	572	576	111	350	2.68
<b>4</b>	469	557	497	609	619	116	390	1.58
<b>5</b>	463	539	522	608	623	108	390	1.86

<sup>a</sup> Luminescence decay lifetimes of compounds 3-5 were performed in dichloromethane solution

Table. 2

Solvent	<b>3</b>				<b>4</b>				<b>5</b>			
	$\lambda_{\text{abs}}/\text{nm}$	$\lambda_{\text{em}}/\text{nm}$	$\Delta\nu/\text{cm}^{-1}$	$^a\Phi_{\text{F}}(\%)$	$\lambda_{\text{abs}}/\text{nm}$	$\lambda_{\text{em}}/\text{nm}$	$\Delta\nu/\text{cm}^{-1}$	$^a\Phi_{\text{F}}(\%)$	$\lambda_{\text{abs}}/\text{nm}$	$\lambda_{\text{em}}/\text{nm}$	$\Delta\nu/\text{cm}^{-1}$	$^a\Phi_{\text{F}}(\%)$
Toluene	445	515	3054	0.765	464	544	3169	0.171	458	560	3977	0.069
CH <sub>2</sub> Cl <sub>2</sub>	439	542	4329	0.732	469	556	3336	0.014	463	539	3045	0.01
THF	437	538	4296	0.703	462	543	3229	0.017	456	524	2846	0.012
EA	434	535	4350	0.707	459	557	3833	0.018	455	535	3286	0.012
DMF	435	556	5003	0.619	460	559	3850	0.28	436	545	4587	0.16

<sup>a</sup> Absolute Quantum yields  $\Phi_{\text{F}}$  was determined in absorption maximum ( $10^{-6}$  M/L) corresponding to the solvents

**Table. 3**

Compds	CV(V)		<sup>a</sup> Energy(eV)-Exp			<sup>b</sup> Eg <sup>opt</sup>
	E <sub>ox/onset</sub>	E <sub>red/onset</sub>	E <sub>HOMO</sub>	E <sub>LUMO</sub>	Eg	
<b>3</b>	0.97	-1.38	-5.67	-3.32	2.35	2.37
<b>4</b>	0.99	-1.30	-5.69	-3.40	2.29	2.15
<b>5</b>	0.96	-1.36	-5.66	-3.34	2.32	2.15

<sup>a</sup> Electronic structure were determined from the below formula: E<sub>HOMO</sub> = -(E<sub>ox</sub> + 4.7) (eV) and E<sub>LUMO</sub> = -(E<sub>red</sub> + 4.7) (eV), <sup>b</sup> Eg<sup>opt</sup> = 1240/λ (absorption band edge)

Table 4

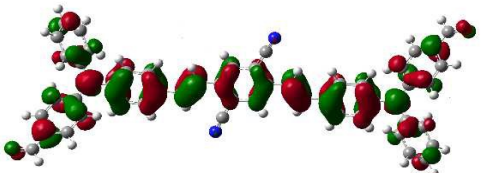
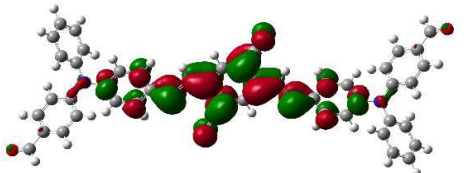
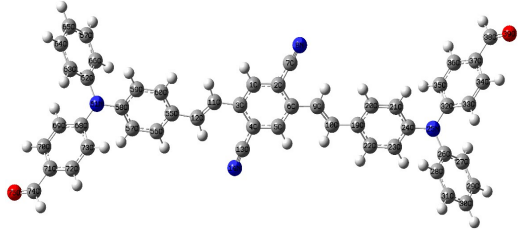
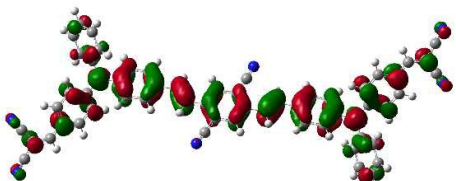
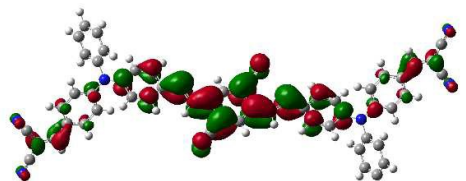
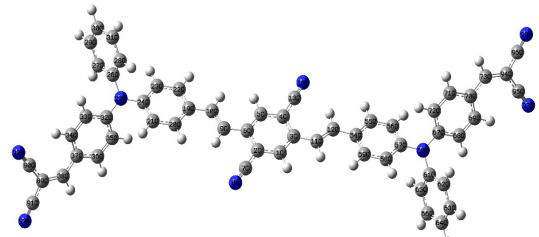
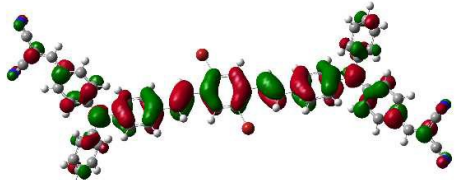
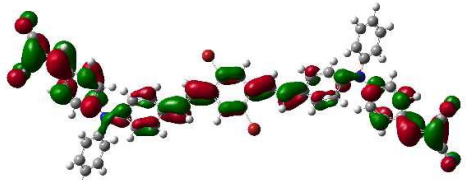
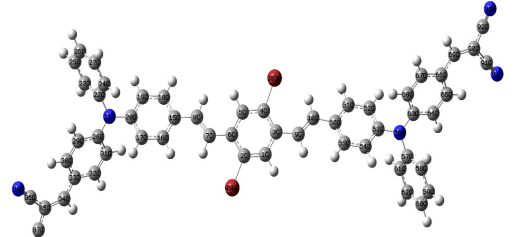
Compd	$E_{\text{HOMO}}$	$E_{\text{LUMO}}$	Steric Structure
3	-5.28 eV 	-3.01 eV 	
4	-5.58 eV 	-3.13 eV 	
5	-5.46 eV 	-3.02 eV 	

Table. 5

3		4		5	
<b>bond length</b>					
O <sub>39</sub> -C <sub>38</sub>	1.22	N <sub>92</sub> -C <sub>90</sub>	1.16	C <sub>86</sub> -N <sub>88</sub>	1.16
C <sub>38</sub> -C <sub>37</sub>	1.47	C <sub>90</sub> -C <sub>89</sub>	1.43	C <sub>86</sub> -C <sub>85</sub>	1.43
C <sub>32</sub> -N <sub>25</sub>	1.41	C <sub>89</sub> -C <sub>38</sub>	1.37	C <sub>85</sub> -C <sub>34</sub>	1.37
C <sub>26</sub> -N <sub>25</sub>	1.43	C <sub>38</sub> -C <sub>37</sub>	1.44	C <sub>34</sub> -C <sub>33</sub>	1.44
C <sub>24</sub> -N <sub>25</sub>	1.42	C <sub>32</sub> -N <sub>25</sub>	1.40	C <sub>28</sub> -N <sub>21</sub>	1.40
C <sub>10</sub> -C <sub>19</sub>	1.46	C <sub>26</sub> -N <sub>25</sub>	1.43	C <sub>22</sub> -N <sub>21</sub>	1.43
C <sub>9</sub> -C <sub>10</sub>	1.35	C <sub>24</sub> -N <sub>25</sub>	1.42	C <sub>20</sub> -N <sub>21</sub>	1.42
C <sub>6</sub> -C <sub>9</sub>	1.46	C <sub>10</sub> -C <sub>19</sub>	1.46	C <sub>15</sub> -C <sub>8</sub>	1.46
C <sub>2</sub> -C <sub>7</sub>	1.43	C <sub>9</sub> -C <sub>10</sub>	1.35	C <sub>8</sub> -C <sub>7</sub>	1.35
C <sub>7</sub> -N <sub>8</sub>	1.16	C <sub>6</sub> -C <sub>9</sub>	1.46	C <sub>7</sub> -C <sub>6</sub>	1.46
		C <sub>2</sub> -C <sub>7</sub>	1.43	C <sub>2</sub> -Br <sub>95</sub>	1.92
		C <sub>7</sub> -N <sub>8</sub>	1.16		
<b>bond angle</b>					
O <sub>39</sub> -C <sub>38</sub> -C <sub>37</sub>	124.91	C <sub>90</sub> -C <sub>89</sub> -C <sub>38</sub>	125.18	C <sub>86</sub> -C <sub>85</sub> -C <sub>84</sub>	125.18
C <sub>24</sub> -N <sub>25</sub> -C <sub>26</sub>	119.01	C <sub>89</sub> -C <sub>38</sub> -C <sub>37</sub>	131.70	C <sub>34</sub> -C <sub>33</sub> -C <sub>32</sub>	117.33
C <sub>26</sub> -N <sub>25</sub> -C <sub>32</sub>	119.75	C <sub>24</sub> -N <sub>25</sub> -C <sub>26</sub>	118.34	C <sub>20</sub> -N <sub>21</sub> -C <sub>22</sub>	118.24
C <sub>24</sub> -N <sub>25</sub> -C <sub>32</sub>	121.24	C <sub>26</sub> -N <sub>25</sub> -C <sub>32</sub>	120.09	C <sub>22</sub> -N <sub>21</sub> -C <sub>28</sub>	120.40
C <sub>9</sub> -C <sub>10</sub> -C <sub>19</sub>	126.95	C <sub>24</sub> -N <sub>25</sub> -C <sub>32</sub>	121.57	C <sub>20</sub> -N <sub>21</sub> -C <sub>28</sub>	121.36
C <sub>6</sub> -C <sub>9</sub> -C <sub>10</sub>	126.40	C <sub>9</sub> -C <sub>10</sub> -C <sub>19</sub>	126.87	C <sub>7</sub> -C <sub>8</sub> -C <sub>15</sub>	126.72
		C <sub>6</sub> -C <sub>9</sub> -C <sub>10</sub>	126.38	C <sub>6</sub> -C <sub>7</sub> -C <sub>8</sub>	126.04
<b>dihedral angle</b>					
C <sub>23</sub> -C <sub>24</sub> -C <sub>26</sub> -C <sub>28</sub>	-73.80	C <sub>23</sub> -C <sub>24</sub> -C <sub>26</sub> -C <sub>28</sub>	-78.71	C <sub>19</sub> -C <sub>20</sub> -C <sub>22</sub> -C <sub>24</sub>	-79.64
C <sub>21</sub> -C <sub>24</sub> -C <sub>32</sub> -C <sub>35</sub>	-63.10	C <sub>21</sub> -C <sub>24</sub> -C <sub>32</sub> -C <sub>35</sub>	-61.26	C <sub>17</sub> -C <sub>20</sub> -C <sub>28</sub> -C <sub>31</sub>	-62.31
C <sub>27</sub> -C <sub>26</sub> -C <sub>32</sub> -C <sub>33</sub>	-71.24	C <sub>27</sub> -C <sub>26</sub> -C <sub>32</sub> -C <sub>33</sub>	-69.32	C <sub>23</sub> -C <sub>22</sub> -C <sub>28</sub> -C <sub>29</sub>	-67.80
C <sub>9</sub> -C <sub>10</sub> -C <sub>19</sub> -C <sub>20</sub>	2.67	C <sub>9</sub> -C <sub>10</sub> -C <sub>19</sub> -C <sub>20</sub>	2.01	C <sub>16</sub> -C <sub>15</sub> -C <sub>8</sub> -C <sub>7</sub>	5.57
C <sub>5</sub> -C <sub>6</sub> -C <sub>9</sub> -C <sub>10</sub>	2.20	C <sub>5</sub> -C <sub>6</sub> -C <sub>9</sub> -C <sub>10</sub>	1.10	C <sub>5</sub> -C <sub>6</sub> -C <sub>7</sub> -C <sub>8</sub>	13.93

Scheme 1

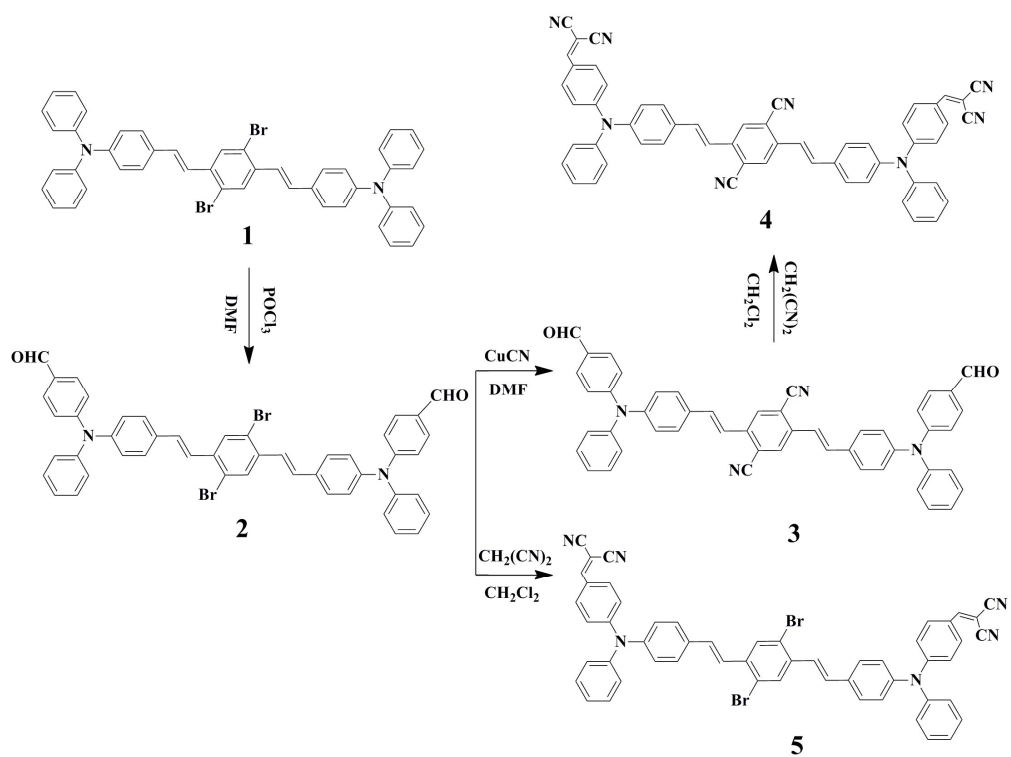


Fig.1

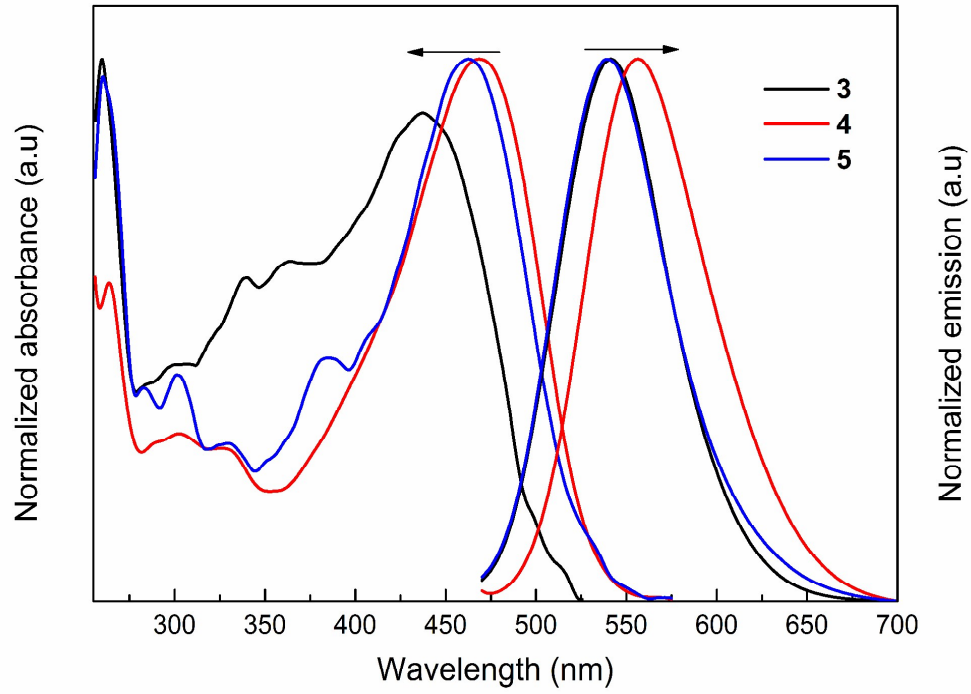


Fig.2

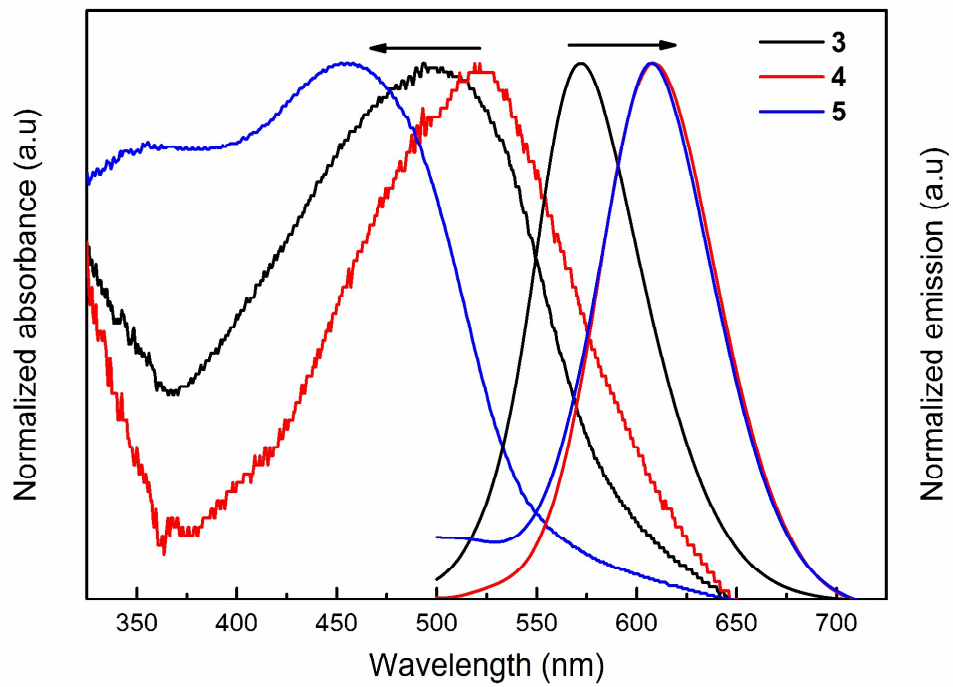


Fig.3

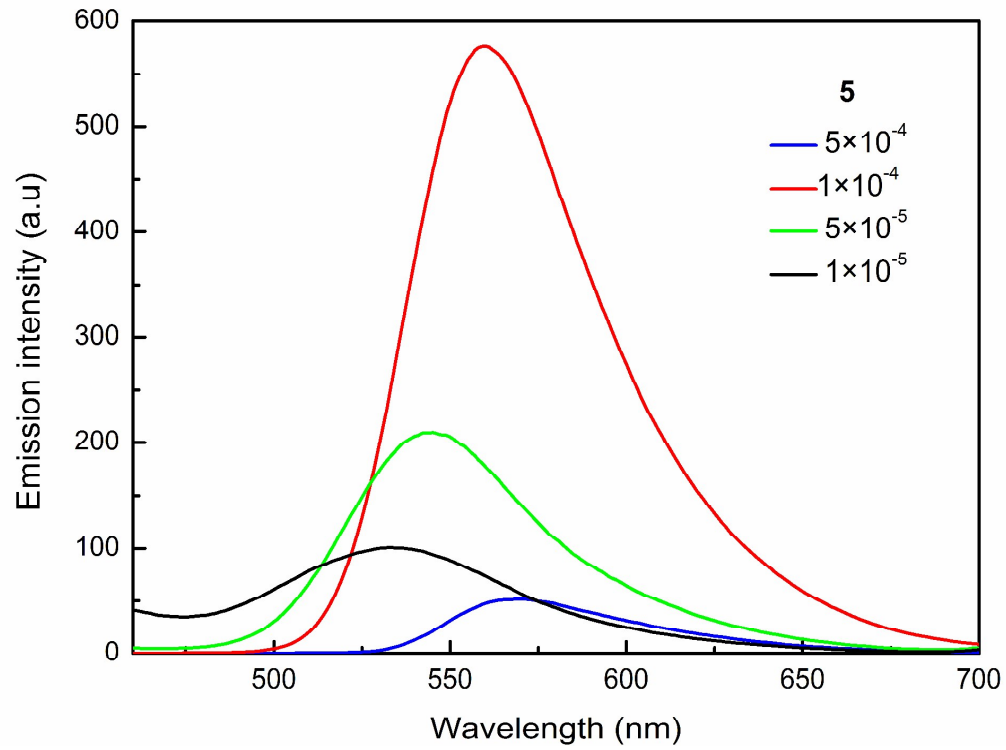
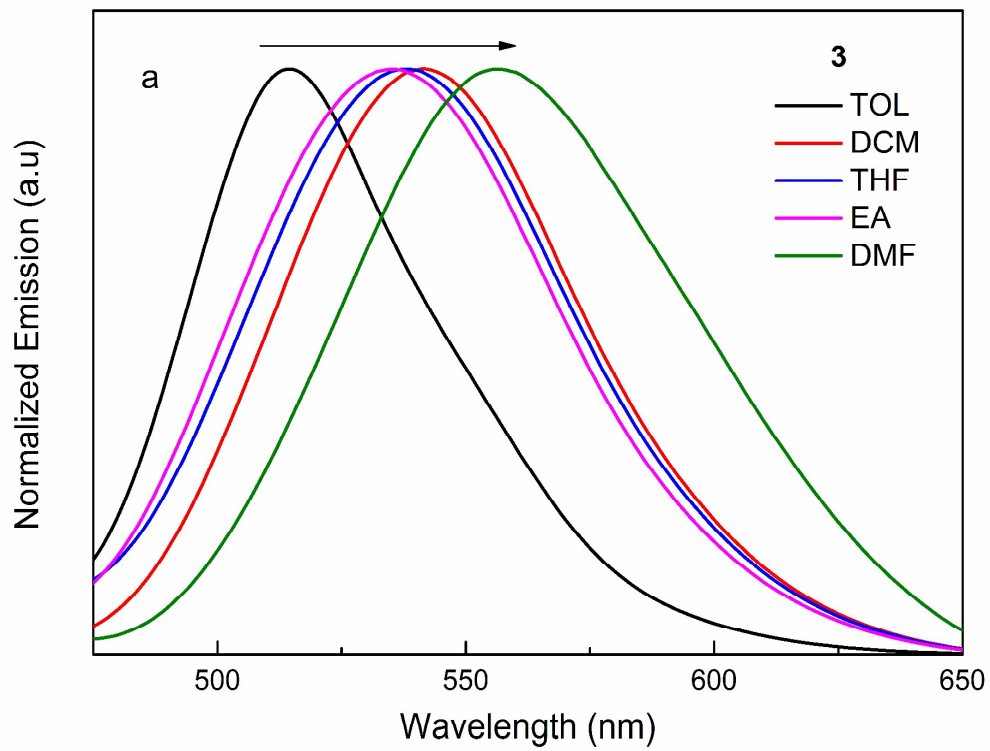
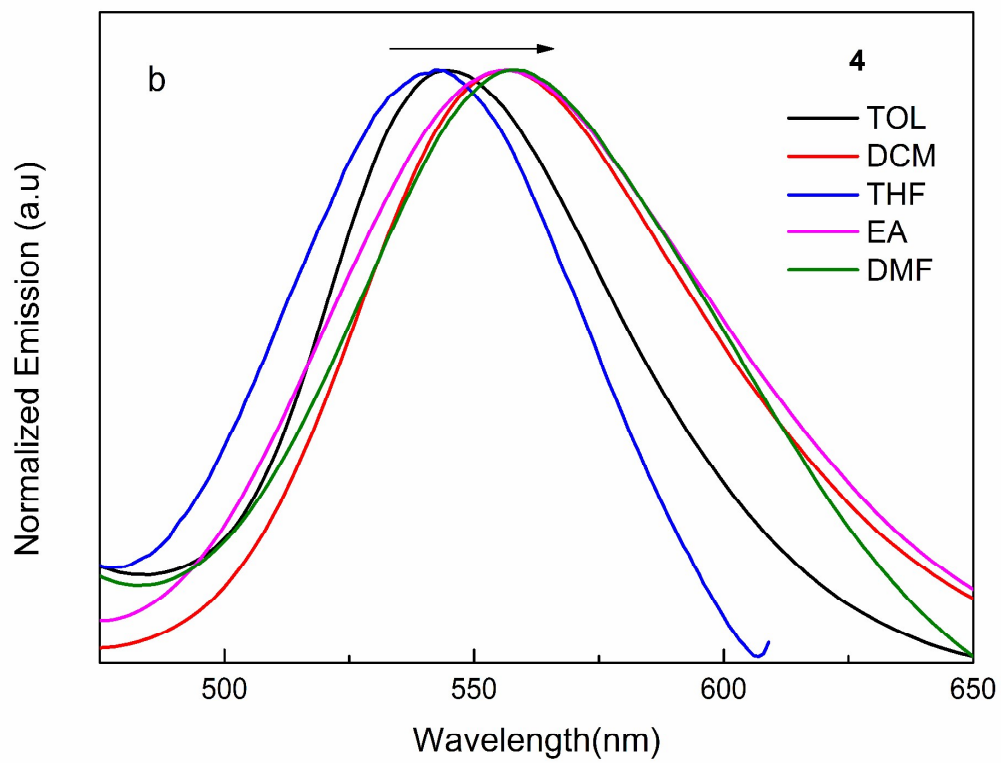
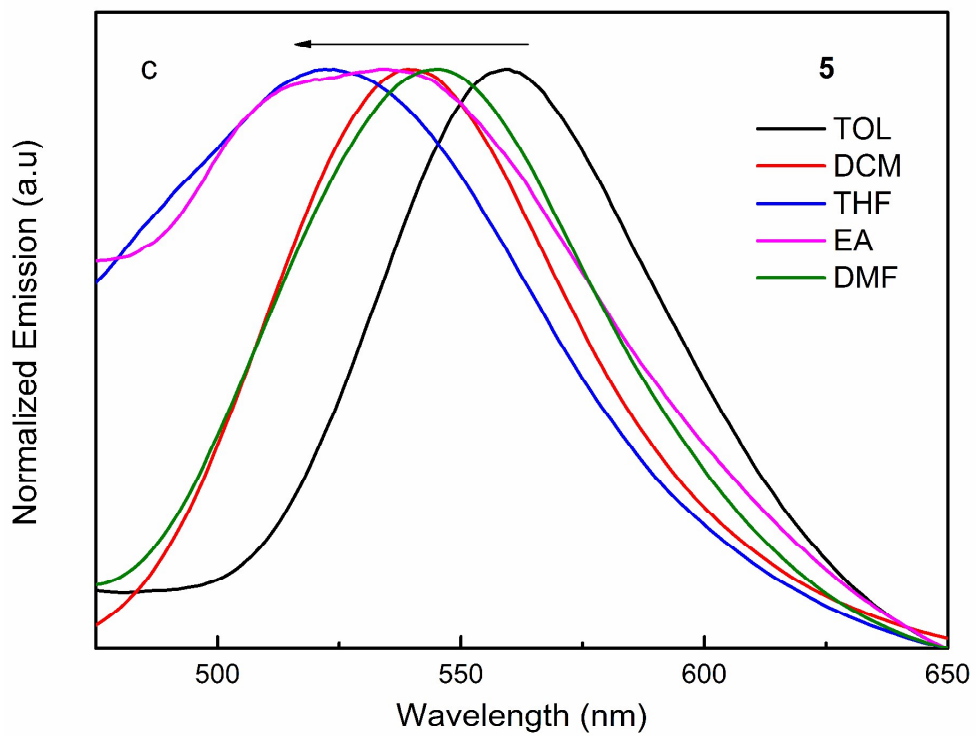


Fig.4







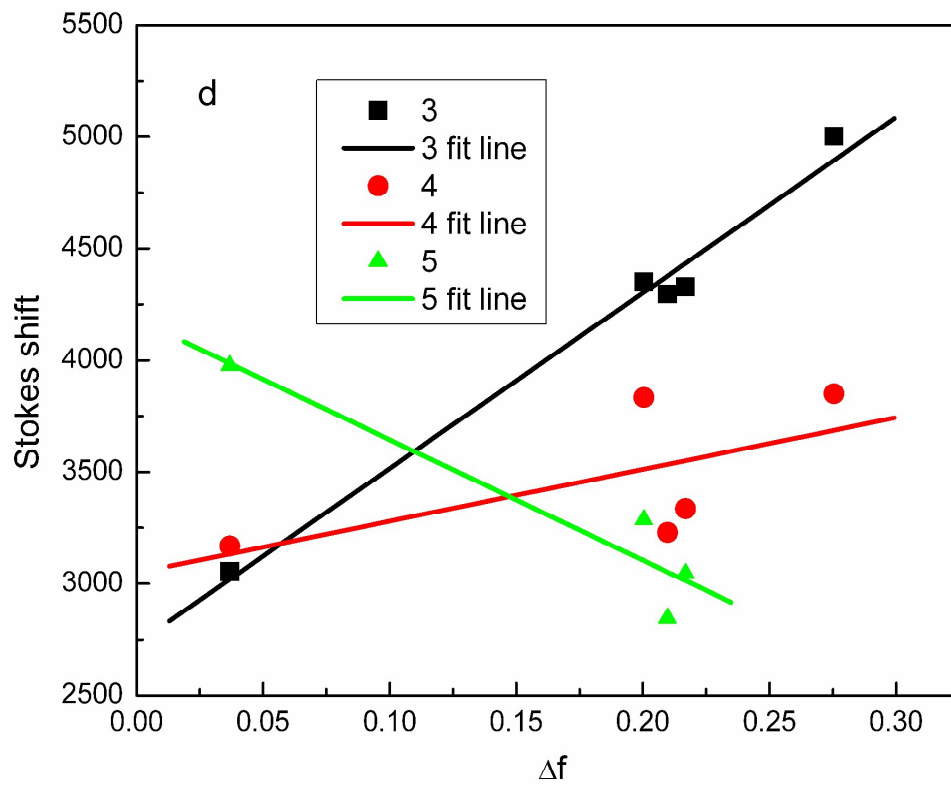
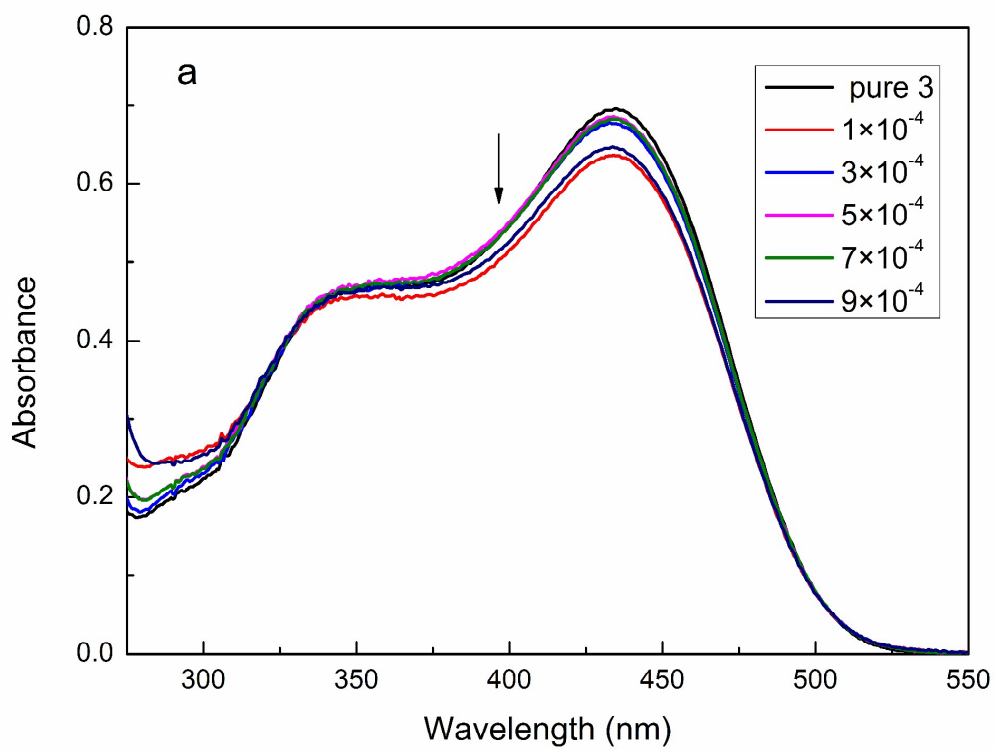
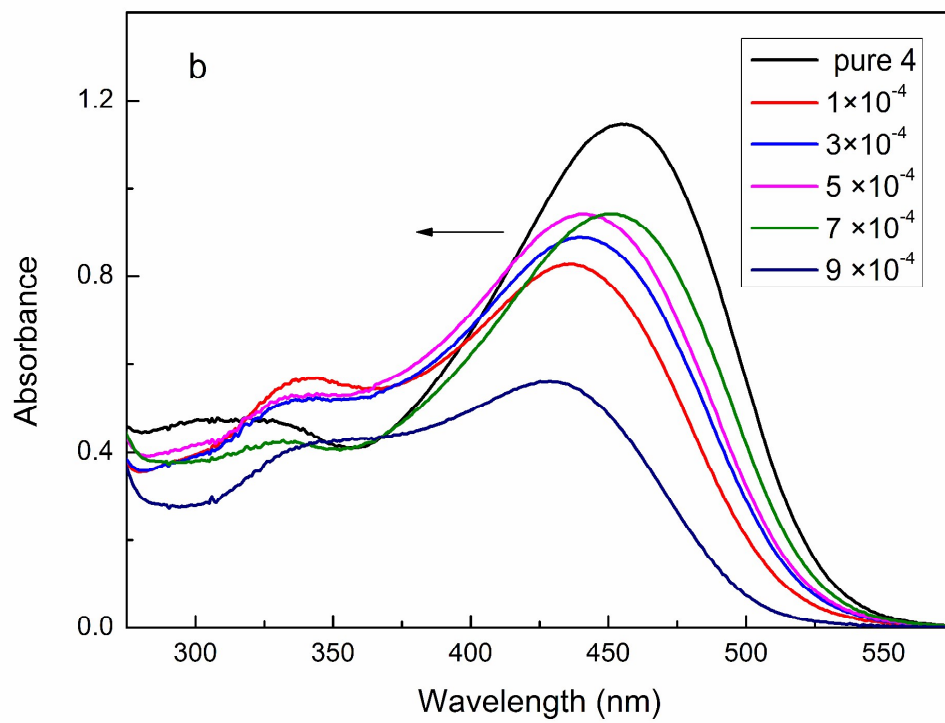


Fig.5





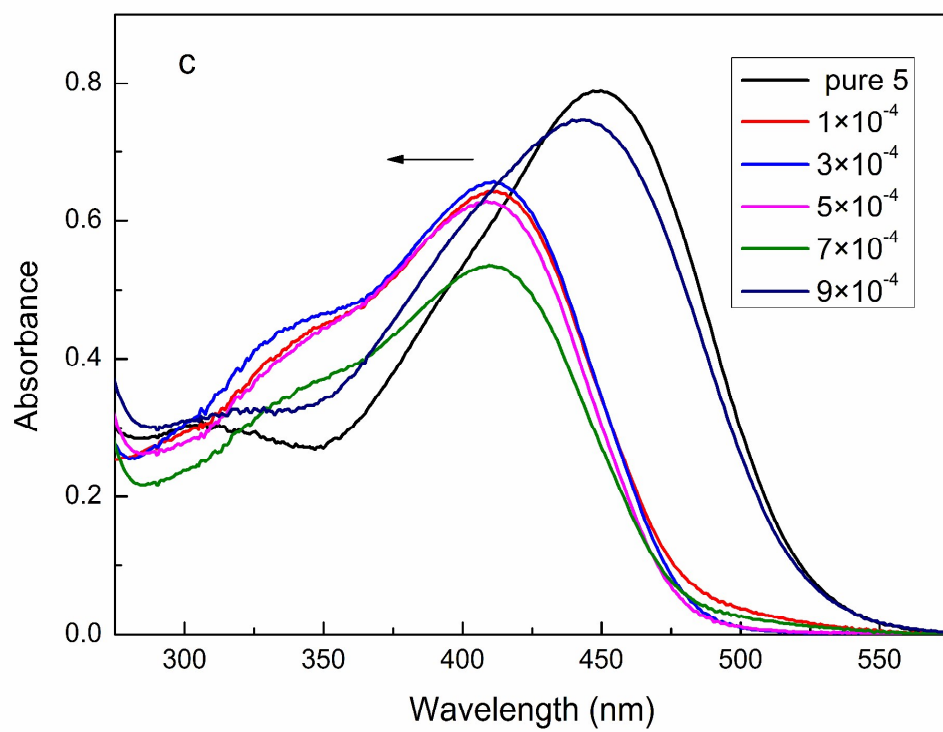


Fig.6

